REPORT DOCUMENTATION PAGE

Form Approved OMB NO. 0704-0188

1. REPORT DATE (DD-MM-YYYY)	2. REPORT TYPE	3. DATES COVERED (From - To)
05-04-2021	Final Report	15-May-2017 - 30-Nov-2020

4. TITLE AND SUBTITLE
Final Report: Ultrafast Chemical Dynamics on Complex, Excited State Energy Landscapes

5a. CONTRACT NUMBER
W911NF-17-1-0256

5b. GRANT NUMBER

5c. PROGRAM ELEMENT NUMBER
611102

6. AUTHORS

5d. PROJECT NUMBER

5e. TASK NUMBER

5f. WORK UNIT NUMBER

7. PERFORMING ORGANIZATION NAMES AND ADDRESSES
Brown University
Office of Sponsored Projects
Box 1929
Providence, RI 02912 -9093

8. PERFORMING ORGANIZATION REPORT NUMBER

9. SPONSORING/MONITORING AGENCY NAME(S) AND ADDRESS (ES)
U.S. Army Research Office
P.O. Box 12211
Research Triangle Park, NC 27709-2211

10. SPONSOR/MONITOR'S ACRONYM(S)
ARO

11. SPONSOR/MONITOR'S REPORT NUMBER(S)
68747-CH.13

12. DISTRIBUTION AVAILIBILITY STATEMENT
Approved for public release; distribution is unlimited.

13. SUPPLEMENTARY NOTES
The views, opinions and/or findings contained in this report are those of the author(s) and should not contrued as an official Department of the Army position, policy or decision, unless so designated by other documentation.

14. ABSTRACT

15. SUBJECT TERMS

16. SECURITY CLASSIFICATION OF:			17. LIMITATION OF ABSTRACT	15. NUMBER OF PAGES	19a. NAME OF RESPONSIBLE PERSON
a. REPORT	b. ABSTRACT	c. THIS PAGE			Peter Weber
UU	UU	UU	UU		19b. TELEPHONE NUMBER 401-863-1007

RPPR Final Report
as of 28-Apr-2021

Agency Code: 21XD

Proposal Number: 68747CH **Agreement Number: W911NF-17-1-0256**
INVESTIGATOR(S):

Name: Peter Weber
Email: peter_weber@brown.edu
Phone Number: 4018631007
Principal: Y

Organization: **Brown University**
Address: Office of Sponsored Projects, Providence, RI 029129093
Country: USA
DUNS Number: 001785542 EIN: 050258809
Report Date: 28-Feb-2021 Date Received: 05-Apr-2021
Final Report for Period Beginning 15-May-2017 and Ending 30-Nov-2020
Title: Ultrafast Chemical Dynamics on Complex, Excited State Energy Landscapes
Begin Performance Period: 15-May-2017 **End Performance Period:** 30-Nov-2020
Report Term: 0-Other
Submitted By: Peter Weber Email: peter_weber@brown.edu
Phone: (401) 863-1007
Distribution Statement: 1-Approved for public release; distribution is unlimited.

STEM Degrees: 3 **STEM Participants:** 8

Major Goals: The project explores the structures and the time-resolved chemical dynamics of important molecular systems in excited states. Two complementary techniques are developed and applied to representative model systems that illustrate a wide range of ultrafast chemical dynamics processes.
Understanding the structures and chemical dynamics of molecules in their excited states is of great importance for basic science and myriad applications within and outside of Chemistry. The project develops two experimental tools and applies them to important molecular systems. Because the experimental methods are complementary, their simultaneous application to the same systems provides deeper insights into the molecular dynamics than each technique would give in isolation.
The experimental methods are ultrafast time resolved gas x-ray diffraction, which is performed at SLAC's LCLS light source, and time-resolved Rydberg fingerprint spectroscopy. All these methods measure the structures of molecules in excited states, with a time resolution of <100 fs for both the x-ray diffraction and the Rydberg spectroscopy. The Rydberg Fingerprint Spectroscopy method has been developed with ARO funding in a prior period. The molecular systems to be studied include: the ring-opening reaction of 1,3-cyclohexadiene, where we seek to observe, over a broad range of excitation energies, the structure of the molecule as it passes the conical intersections; the conformeric structure and dynamics of N-methyl morpholine, which features fascinating conformeric relaxation dynamics; and the effect of solvation on the charge delocalization of tertiary amines.
By focusing on structurally well-defined molecules and molecular clusters, the project advances our knowledge of molecules in excited electronic states, their chemical dynamics, and the effect of solvent environments. This aids numerous applications and is also valuable to the continued development of computational methods.
Successful outcome of the proposed work results in a better understanding of molecular structures and chemical dynamics in excited states. The excited state structures provide experimental benchmarks that are needed for the development of computational methods. The research resulted in publications that inform the scientific community.

Accomplishments: In this period, we focused on the specific goal of determining excited state structures using X-ray scattering. As a first step, we carefully analyzed contributions to the scattering patterns that arise from different phenomena. A detailed understanding of these effects is required if one wishes to determine accurate structures for molecules in excited and short lived states far from their equilibrium geometry.

For polyatomic molecular systems, large amplitude vibrational motions are associated with anharmonicity and shifts of interatomic distances, making analytical solutions using traditional harmonic approximations inapplicable. More generally, the interatomic distances in a polyatomic molecule are not independent and the traditional equations commonly used to interpret the data may give unphysical results.

We developed a novel method based on molecular dynamic trajectories and applied it to two examples of hot, vibrating molecules at thermal equilibrium. When excited at 200 nm, 1,3-cyclohexadiene (CHD) relaxes on a subpicosecond time scale back to the reactant molecule, the dominant pathway, and to various forms of 1,3,5-hexatriene (HT). With internal energies of about 6 eV, the energy thermalizes quickly, leading to structure distributions that deviate significantly from their vibrationless equilibrium.

The experimental and theoretical results are in excellent agreement and reveal that a significant contribution to the scattering signal arises from transition state structures near the inversion barrier of CHD. In HT, our analysis clarifies that previously inconsistent structural parameters determined by other researchers using electron diffraction were artifacts that might have resulted from the use of inapplicable analytical equations.

We also have carefully analyzed scattering patterns of a molecular system with charge transfer. We are able to extract molecular structures of species with different charge distributions with precision rivaling ground state structure determinations.

Training Opportunities: A total of seven graduate students were participating in the research of the group, even though many were funded through other means. Students receive one-on one training from the PI in the laboratory, or remotely during extended discussion sessions. Students also participate in weekly group meetings where results are presented and discussed. Students furthermore participate in experiments with our collaborators and at National Labs as opportunities arise.

Students give frequent talks at our weekly group meeting and an annual talk to a departmental audience to present their research and results. During the Covid pandemic times, all group meetings and seminars were held by video.

Several students attended a week-long summer school at SLAC National Laboratory.

Students also benefited from the presence of a post doc from Europe.

Before the pandemic hit, students participated in conferences to present their research results. Unfortunately, both travel and lab work was interrupted starting in March of 2020.

Results Dissemination: The research resulted in seven publications within the current reporting period (see listing under 'products').

The results of the research were moreover presented in informal ways in the courses I teach at Brown University. In particular, they flow into a freshman seminar that is attended by students from all disciplines and who would not traditionally take a chemistry course. They also feature in a graduate level quantum mechanics course that I teach.

Finally, the results were presented at 15 national and international conferences.

Honors and Awards: Nothing to Report

Protocol Activity Status:

Technology Transfer: Nothing to Report

PARTICIPANTS:

Participant Type: PD/PI
Participant: Peter M Weber Dr
Person Months Worked: 1.00 **Funding Support:**
Project Contribution:
National Academy Member: N

RPPR Final Report
as of 28-Apr-2021

ARTICLES:

Publication Type: Journal Article Peer Reviewed: Y **Publication Status:** 1-Published
Journal: Russian Chemical Review
Publication Identifier Type: DOI Publication Identifier: 10.1070/RCR4754
Volume: 86 Issue: 12 First Page #: 1173
Date Submitted: 7/26/18 12:00AM Date Published: 12/1/17 5:00AM
Publication Location:
Article Title: Transient structures and chemical reaction dynamics
Authors: Anatoly A. Ischenko, Peter M. Weber and R. J. Dwayne Miller
Keywords: X-ray scattering; electron scattering; ultrafast; molecular reaction dynamics; time resolved
Abstract: To study transition structures that are formed in real time during a chemical reaction process, it is necessary to use ultrafast methods to follow the structural dynamics of molecular systems. For many decades, optical methods have been used to study the electronic states and time course giving rise to structural intermediates of chemical reactions with an ever higher time resolution. Although in some cases optical methods show many details, ultimately the results of these observations give only indirect information about the structure of the chemical reaction intermediates. Experimental observation of the behaviour of matter in the space-time continuum on ultrashort time scale is the necessary first step to explain and, subsequently, to control the nonequilibrium processes and functionality of the systems under study, to trace the relationship between the elements of the triad `Structure ± Dynamics ± Function' to fully understand material properties. The results of these studies ...
Distribution Statement: 3-Distribution authorized to U.S. Government Agencies and their contractors
Acknowledged Federal Support: **Y**

Publication Type: Journal Article Peer Reviewed: Y **Publication Status:** 1-Published
Journal: Physical Chemistry Chemical Physics
Publication Identifier Type: DOI Publication Identifier: 10.1039/c7cp05244h
Volume: 19 Issue: First Page #: 26403
Date Submitted: 7/26/18 12:00AM Date Published: 9/14/17 4:00AM
Publication Location:
Article Title: Coherence in Nonradiative Transitions: Internal Conversion in Rydberg-Excited N-Methyl and N-Ethyl Morpholine
Authors: Yao Zhang, Hannes Jónsson, Peter M. Weber
Keywords: Coherence; electronic relaxation; reaction dynamics; ultrafast
Abstract: The survival of coherent wavepacket motion during internal conversions is observed in relatively large molecules, N-methyl morpholine and N-ethyl morpholine, where standard models imply fast decoherence in a statistical limit. Optical excitation in the region of 194 to 230 nm excites the molecule to 3s or 3p Rydberg states, launching a wavepacket motion in the umbrella mode of the tertiary amine chromophore. In the short wavelength range, o214 nm, the molecules are excited to the 3p Rydberg state, which decays by internal conversion on a time scale of about 100 fs to the lower-lying 3s Rydberg state. Time- resolved photoionization photoelectron experiments reveal that the coherent wavepacket motion survives the internal conversion with oscillations continuing in the 3s state for several 650 fs periods before the phase lock is lost due to dephasing into the dense bath of vibrational modes of the molecule.
Distribution Statement: 3-Distribution authorized to U.S. Government Agencies and their contractors
Acknowledged Federal Support: **Y**

RPPR Final Report
as of 28-Apr-2021

Publication Type: Journal Article Peer Reviewed: Y **Publication Status:** 1-Published
Journal: Optics Letters
Publication Identifier Type: DOI Publication Identifier: 10.1364/OL.43.001279
Volume: 43 Issue: 6 First Page #: 1279
Date Submitted: 7/26/18 12:00AM Date Published: 2/15/18 5:00AM
Publication Location:
Article Title: Spatially resolved standoff trace chemical sensing using backwards transient absorption spectroscopy
Authors: Fedor Rudakov, Joseph D. Geiser and Peter M. Weber
Keywords: DIAL, differential absorption lidar; Remote sensing and sensors; Backscattering; Absorption; Spectroscopy, laser; Spectroscopy, coherent transient.
Abstract: A technique for the spatially resolved and molecule-specific detection of chemical vapors is presented. The chemical specificity arises from a transient absorption spectrum where an ultraviolet (UV) pulse excites the molecule to a Rydberg state, and a near-infrared (NIR) or visible probe pulse records a transient absorption spectrum. By record- ing the NIR pulse reflected off a random, distant object and measuring the elapsed time between the emission of the UV pulse and the absorption of a counter-propagating NIR pulse, the distance to the absorber is obtained. The feasibility of the approach is demonstrated by detecting acetone plumes with millimeter scale spatial resolu- tion.
Distribution Statement: 3-Distribution authorized to U.S. Government Agencies and their contractors
Acknowledged Federal Support: **Y**

Publication Type: Journal Article Peer Reviewed: Y **Publication Status:** 1-Published
Journal: Journal of Chemical Physics
Publication Identifier Type: DOI Publication Identifier: 10.1063/1.5031787
Volume: 148 Issue: First Page #: 194306
Date Submitted: 7/26/18 12:00AM Date Published: 5/21/18 8:00AM
Publication Location:
Article Title: Ultrafast photodissociation dynamics of 1,4-diiodobenzene
Authors: Brian Stankus, Nikola Zotev, David M. Rogers, Yan Gao, Asami Odate, Adam Kirrander and Peter M. W
Keywords: Chemical dynamics; reaction dynamics; ultrafast; photodissociation
Abstract: The photodissociation dynamics of 1,4-diiodobenzene is investigated using ultrafast time-resolved photoelectron spectroscopy. Following excitation by laser pulses at 271 nm, the excited-state dynamics is probed by resonance-enhanced multiphoton ionization with 405 nm probe pulses. A progression of Rydberg states, which come into resonance sequentially, provide a fingerprint of the dissoci- ation dynamics of the molecule. The initial excitation decays with a lifetime of 33 ± 4 fs, in good agreement with a previous study. The spectrum is interpreted by reference to ab initio cal- culations at the CASPT2(18,14) level, including spin-orbit coupling. We propose that both the 5B1 and 6B1 states are excited initially, and based on the calculations, we identify diabatic spin- orbit coupled states corresponding to the main dissociation pathways.
Distribution Statement: 3-Distribution authorized to U.S. Government Agencies and their contractors
Acknowledged Federal Support: **Y**

RPPR Final Report
as of 28-Apr-2021

Publication Type: Journal Article Peer Reviewed: Y **Publication Status:** 1-Published
Journal: Physical Chemistry Chemical Physics
Publication Identifier Type: DOI Publication Identifier: 10.1039/C8CP05950K
Volume: 21 Issue: 5 First Page #: 2283
Date Submitted: 7/18/19 12:00AM Date Published:
Publication Location:
Article Title: Symmetry controlled excited state dynamics
Authors: Max D. J. Waters, Anders B. Skov, Martin A. B. Larsen, Christian M. Clausen, Peter M. Weber, Theis I.
Keywords: Coherence, ultrafast molecular dynamics, dephasing, internal conversion
Abstract: Symmetry effects in internal conversion are studied by means of two isomeric cyclic tertiary aliphatic amines in a velocity map imaging (VMI) experiment on the femtosecond timescale. It is demonstrated that there is a delicate structural dependence on when coherence is preserved after the transition between the 3p and 3s Rydberg states. N-Methyl morpholine (NMM) shows unambiguous preserved coherence, consistent with previous work, which is decidedly switched off by the repositioning of oxygen within the ring. From the differences in these dynamics, and an examination of the potential energy surface following the normal modes of vibration, it becomes clear that there is a striking dependence on atom substitution, which manifests itself in the permitted modes of vibration that take the system out of the Franck–Condon region through to the 3s minimum. It is shown that the non Fermi-like behaviour of NMM is due to a conical intersection (CI) between the 3px and 3s states lying directly ...
Distribution Statement: 3-Distribution authorized to U.S. Government Agencies and their contractors
Acknowledged Federal Support: **Y**

Publication Type: Journal Article Peer Reviewed: Y **Publication Status:** 1-Published
Journal: Nature Chemistry
Publication Identifier Type: DOI Publication Identifier: 10.1038/s41557-019-0291-0
Volume: Issue: First Page #:
Date Submitted: 7/18/19 12:00AM Date Published: 7/1/19 4:00AM
Publication Location:
Article Title: Ultrafast X-ray scattering reveals vibrational coherence following Rydberg excitation
Authors: Brian Stankus, Haiwang Yong, Nikola Zotev, Jennifer M. Ruddock, Darren Bellshaw, Thomas J. Lane, M
Keywords: Ultrafast dynamics, molecular structure, coherence
Abstract: The coherence and dephasing of vibrational motions of molecules constitute an integral part of chemical dynamics, influence material properties and underpin schemes to control chemical reactions. Considerable progress has been made in understand- ing vibrational coherence through spectroscopic measurements, but precise, direct measurement of the structure of a vibrating excited-state polyatomic organic molecule has remained unworkable. Here, we measure the time-evolving molecular structure of optically excited N-methylmorpholine through scattering with ultrashort X-ray pulses. The scattering signals are corrected for the differences in electron density in the excited electronic state of the molecule in comparison to the ground state. The experiment maps the evolution of the molecular geometry with femtosecond resolution, showing coherent motion that survives electronic relaxation and seems to persist for longer than previously seen using other methods.
Distribution Statement: 3-Distribution authorized to U.S. Government Agencies and their contractors
Acknowledged Federal Support: **Y**

RPPR Final Report
as of 28-Apr-2021

Publication Type: Journal Article Peer Reviewed: Y **Publication Status:** 1-Published
Journal: Journal of Chemical Physics
Publication Identifier Type: DOI Publication Identifier: doi.org/10.1063/1.5111979
Volume: 151 Issue: First Page #: 084301
Date Submitted: 8/19/20 12:00AM Date Published: 9/9/19 1:35AM
Publication Location:
Article Title: Scattering off Molecules far from Equilibrium
Authors: Haiwang Yong, Jennifer M. Ruddock, Brian Stankus, Lingyu Ma, Wenpeng Du, Nathan Goff, Yu Chang,
Keywords: Ultrafast X-ray scattering
Abstract: Pump-probe gas phase X-ray scattering experiments, enabled by the development of X-ray free electron lasers, have advanced to reveal scattering patterns of molecules far from their equilibrium geometry. While dynamic displacements reflecting the motion of wavepackets can probe deeply into the reaction dynamics, in many systems, the thermal excitation embedded in the molecules upon optical excitation and energy randomization can create systems that encompass structures far from the ground state geometry. For polyatomic molecular systems, large amplitude vibrational motions are associated with anharmonicity and shifts of interatomic distances, making analytical solutions using traditional harmonic approximations inapplicable. More generally, the interatomic distances in a polyatomic molecule are not independent and the traditional equations commonly used to interpret the data may give unphysical results. Here, we introduce a novel method based on molecular dynamic trajectories and illust
Distribution Statement: 1-Approved for public release; distribution is unlimited.
Acknowledged Federal Support: **Y**

DISSERTATIONS:

Publication Type: Thesis or Dissertation
Institution: Brown University
Date Received: 18-Jul-2019 Completion Date: 5/18/19 8:52PM
Title: Ultrafast Chemical Dynamics: Photochemistry in Real Time
Authors: Brian Stankus
Acknowledged Federal Support: **N**

Publication Type: Thesis or Dissertation
Institution: Brown University
Date Received: 19-Aug-2020 Completion Date: 8/19/19 9:37PM
Title: Ultrafast Kinetics Analysis of Gas-Phase Reactions using Ultrafast X-Ray Scattering
Authors: Jennifer M. Ruddock
Acknowledged Federal Support: **N**

Partners

,

RPPR Final Report
as of 28-Apr-2021

I certify that the information in the report is complete and accurate:
Signature:
Signature Date:

nature chemistry

ARTICLES

https://doi.org/10.1038/s41557-019-0291-0

Ultrafast X-ray scattering reveals vibrational coherence following Rydberg excitation

Brian Stankus[1,4], Haiwang Yong[1,4], Nikola Zotev[2], Jennifer M. Ruddock[1], Darren Bellshaw[2], Thomas J. Lane[3], Mengning Liang[3], Sébastien Boutet[3], Sergio Carbajo[3], Joseph S. Robinson[3], Wenpeng Du[1], Nathan Goff[1], Yu Chang[1], Jason E. Koglin[3], Michael P. Minitti[3], Adam Kirrander[2] and Peter M. Weber[1*]

The coherence and dephasing of vibrational motions of molecules constitute an integral part of chemical dynamics, influence material properties and underpin schemes to control chemical reactions. Considerable progress has been made in understanding vibrational coherence through spectroscopic measurements, but precise, direct measurement of the structure of a vibrating excited-state polyatomic organic molecule has remained unworkable. Here, we measure the time-evolving molecular structure of optically excited *N*-methylmorpholine through scattering with ultrashort X-ray pulses. The scattering signals are corrected for the differences in electron density in the excited electronic state of the molecule in comparison to the ground state. The experiment maps the evolution of the molecular geometry with femtosecond resolution, showing coherent motion that survives electronic relaxation and seems to persist for longer than previously seen using other methods.

The coherence of molecular vibrations—and its decay by dephasing—determines a wide array of molecular properties and governs the widths and shapes of observed vibrational spectral lines[1,2]. Statistical theories for chemical reactions assume that dephasing leads to the dissipation of vibrational energy throughout the available phase space[3]. Dephasing could thus be considered an obstacle to the coherent control of chemical reaction dynamics using laser pulses[4] and to other fields that rely on the quantum coherence of molecular vibrations.

The advent of ultrashort pulsed optical lasers ushered in a new era of femtochemistry. Femtosecond laser pulses allowed spectroscopic measurements of time-evolving molecules in real time, providing intriguing glimpses of the intricate ways in which molecular excitation can lead to chemical dynamics and vibrational coherences[5,6]. These ultrafast studies, which rely on spectroscopic probes, have generated a wealth of knowledge about photochemical reaction mechanisms. Yet, spectroscopy is an inherently indirect probe of structural dynamics, and so following the dephasing of polyatomic molecules in real time—at the level of individual bond parameters—remains challenging.

With the recent advent of ultrafast X-ray free-electron lasers and ultrafast electron diffraction, more direct measurements of time-dependent atomic positions have become possible[7–15]. Ultrafast gas-phase scattering has emerged as a powerful tool for measuring molecular dynamics[7,8,13,14,16–18], revealing chemical reaction mechanisms that were previously inferred but not observed. In this study, we show that precise excited-state molecular structures can be obtained from X-ray scattering patterns and used to construct a detailed picture of their dynamics with femtosecond time resolution. Recent spectroscopic studies have revealed that in *N*-methylmorpholine (NMM), coherent vibrational motions can survive an electronic relaxation process[19,20]. Here, we show that the low-frequency coherent vibrations of NMM have been clearly resolved in space and time using time-resolved X-ray scattering with ultrafast pulses generated by the Linac Coherent Light Source (LCLS). The determined time-resolved molecular structures show that the coherent motions persist well beyond electronic relaxation. This is an important finding because such electronic relaxation phenomena in large-molecule systems have traditionally been regarded as statistical in nature.

The nature of the initial excited state when NMM is pumped with 200 nm radiation has previously been the subject of investigation. Analysis of the anisotropic X-ray scattering signal of NMM immediately following 200 nm excitation revealed the population of the $3p_z$ molecular Rydberg state[21]. In ultrafast photoelectron spectroscopy studies, excitation to the $3p_z$ state[21] has been seen to launch a coherent structural oscillation that persists following internal conversion to the 3*s* state with a 106 fs time constant[19]. Electronic structure calculations indicate that the molecular structure in the electronic ground state is an equatorial chair structure[20,22] (shown in Fig. 1), and the observed photoelectron signals indicate that the structural motion primarily responsible for the observed oscillation is a coherent vibration in a mode that involves the planarization of the amine, which is consistent with related computational studies on the same molecule[23].

In this work, the transient structures of the molecule as it evolves in time on the Rydberg surface are determined by matching the experimentally measured X-ray scattering patterns against a large set of computed patterns that are from a global geometry search in a conformational space created from molecular dynamics simulations. This analysis, along with a correction to the signals stemming from the change in electron density following excitation, is capable of providing a femtosecond time-resolved determination of electronically excited molecular structures in a polyatomic molecule, even in the absence of heavy elements.

In the experiment, a 200 nm UV pump pulse excited the molecules to the $3p_z$ Rydberg state[19,21] (Fig. 1). The scattering patterns

[1]Department of Chemistry, Brown University, Providence, RI, USA. [2]EaStCHEM, School of Chemistry, University of Edinburgh, Edinburgh, UK. [3]Linac Coherent Light Source, SLAC National Accelerator Laboratory, Menlo Park, CA, USA. [4]These authors contributed equally: Brian Stankus, Haiwang Yong. *e-mail: peter_weber@brown.edu

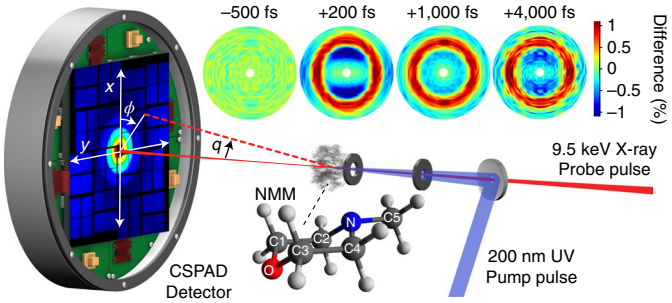

Fig. 1 | A schematic of the experimental set-up. The reaction of NMM is initiated with a 200 nm UV pump pulse, and the time-evolving molecular structure is probed by scattering using 9.5 keV X-ray probe pulses with a variable time delay. The scattering signals are recorded with a CSPAD detector. The percentage change in the scattering pattern as a function of q and Φ for several representative time delays is also shown (top).

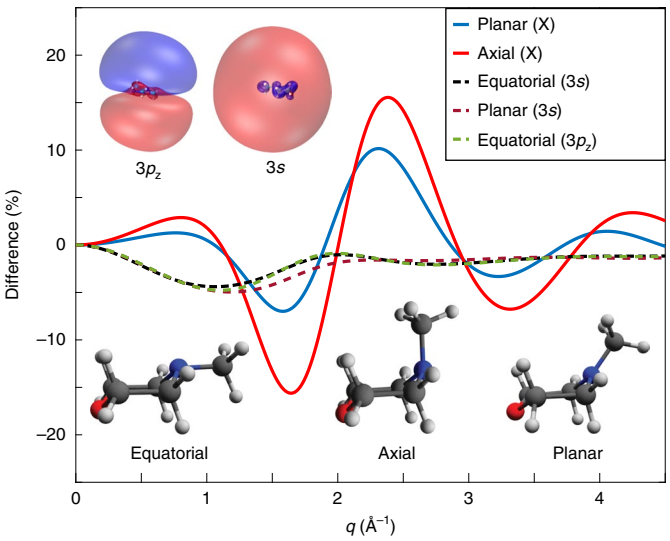

Fig. 2 | The calculated difference in scattering patterns caused by nuclear and electronic structure changes as a function of q. This assumes 100% excitation of the sample. The three relevant molecular conformations, as well as orbital plots for the 3*s* and 3p_z states, are included as insets. The planar (X) (blue solid line) and axial (X) (red solid line) curves are the difference between the planar and equatorial structures in the ground state, and between the axial and equatorial structures in the ground state, respectively. X, the electronic ground state of the molecule. The equatorial (3*s*) (black dashed line) and planar (3*s*) (red dashed line) curves are the difference between the equatorial structure in the 3*s* and ground states, and between the planar structure in the 3*s* and ground states, respectively. The equatorial (3p_z) curve (black dashed line) is the difference between the equatorial structure in the 3p_z and ground states.

created by intersecting the sample with a pulsed, 9.5 keV X-ray beam from the LCLS light source were detected by a 2.3 megapixel Cornell–SLAC pixel array detector (CSPAD)[24]. The positions of the detected X-rays were converted to the coordinates of the amplitude of the scattering vector (q) and the azimuthal angle (ϕ) as described in Supplementary Section 1.

Results and discussion

Experimental results. The time-evolving signals are expressed as a percentage change (equation (1)), where $I_{on}(\phi,q,t)$ represents the scattering pattern at the given time delay (t), and $I_{off}(\phi,q)$ represents the scattering pattern of the ground-state unexcited molecules. The resulting time-dependent scattering images (see Fig. 1 for an illustration; a full animation is provided in Supplementary Video 1) show a sudden onset of the difference signal following optical excitation. An anisotropic component of the signal (seen most clearly at $t = 200$ fs) arises from the preferential excitation of those molecules whose transition dipole moments are oriented parallel to the linear polarization of the optical pump pulse in the laboratory frame. Because the anisotropy is determined by the relationship between the transition dipole moment vector in the initially accessed state and the laser polarization vector, a detailed analysis of this component previously derived an unambiguous assignment of the initially excited state to the 3p_z Rydberg state[21]. The isotropic signal, on the other hand, contains all of the intrinsic information of the molecule in the molecular frame, including both the nuclear and electronic structural evolutions. The two components are decomposed from the two-dimensional scattering patterns using a standard method[25,26]:

$$P_{diff}(\phi,q,t) = 100\frac{I_{on}(\phi,q,t) - I_{off}(\phi,q)}{I_{off}(\phi,q)} \quad (1)$$

The isotropic scattering signal—which shows a time dependence that reveals the dynamics of all internal degrees of freedom of the reacting molecule—has two main features: a rapid 'step function' onset, and a subsequent oscillation that reflects vibrational motions in the molecule and occurs on a timescale that is in good agreement with previous photoelectron studies (623 ± 19 fs versus 630 ± 13 fs measured before)[19] (all errors are reported as 1σ). The oscillation is heavily damped with a time constant of 635 ± 116 fs, which also agrees with the 530 ± 66 fs value measured by photoelectron spectroscopy. A third, low-amplitude exponential-decay feature (see Supplementary Fig. 2) probably arises from intramolecular vibrational relaxation on a picosecond timescale. There is a rapid onset of the difference scattering signal, which is attributed to the electronic transition of NMM from the ground state to the Rydberg state, as well as small-amplitude nuclear motions following electronic excitation. Consequently, the effects of electronic excitation need to be considered to extract the structural motions of the vibrating molecule.

Calculation of electronic excitation effects. The effect on the scattering patterns that results from the change in electron density due to the optical excitation is calculated using ab initio multiconfigurational wavefunctions obtained from the state-averaged complete active-space self-consistent field method (SA5-CASSCF(2,5)/6-311++G(d,p)) (refs. [27,28]). Figure 2 shows the effect of electronic excitation on the scattering signals in comparison to conformational change. The relative magnitude of the effect of the redistribution of electron density following excitation is seen to be approximately half of the effect from the nuclear structure change, depending on the specific molecular geometry. At certain vibrational displacements, the two effects can be nearly comparable in magnitude, meaning that the signatures of both are captured in the scattering experiment. For example, for the planar structure represented in Fig. 2, the electronic contribution has a magnitude of −4.7% difference at $q = 1$ Å^{-1}, whereas the structural contribution has a magnitude of only 0.5%. Clearly, the electronic contribution must be included to adequately account for the observed difference signals.

The effect on the scattering signal that arises from the change in the spatial distribution of the Rydberg electron as it internally converts from 3p_z to 3*s* is not experimentally observed, which is consistent with a very small difference in the calculated effect (Fig. 2). This is because the Rydberg orbitals are very diffuse, and,

Table 1 | The molecular structure parameters of vibrationally hot NMM in the excited 3*s* state, determined for delay times from 2.6 ps to 3.9 ps

	Experimental		Calculated	
	Rydberg-surface dynamics pool	Ion-surface dynamics pool	Ion structure	Ground-state structure
Nearest-neighbour interatomic distances (Å)				
O–C3	1.368 ± 0.005	1.373 ± 0.008	1.401	1.398
O–C1	1.364 ± 0.008	1.374 ± 0.006	1.401	1.398
N–C4	1.434 ± 0.012	1.449 ± 0.007	1.439	1.453
N–C2	1.441 ± 0.019	1.447 ± 0.009	1.439	1.453
N–C5	1.433 ± 0.007	1.430 ± 0.006	1.454	1.446
C3–C4	1.557 ± 0.009	1.554 ± 0.008	1.580	1.519
C2–C1	1.578 ± 0.023	1.552 ± 0.006	1.580	1.519
Characteristic angles (°)				
C2–C1–C4–C3 torsional	0.6 ± 1.5	−0.3 ± 0.5	0.0	0.0
O–N–C5 umbrella	28.3 ± 6.1	20.4 ± 2.7	37.4	−24.1
N–C4–C2–C5 pyramidalization	1.4 ± 1.2	−0.1 ± 1.0	4.0	−17.4
C5–N–C4–C3 torsional	56.8 ± 4.3	44.3 ± 3.1	70.3	1.6

The errors are the s.d. over measurements at different time points.

when rotationally averaged, the difference between them is small. The electronic effect observed in the scattering experiment must therefore primarily arise from the vacancy left in the nitrogen valence orbitals of the tertiary amine group following the promotion of an electron to the Rydberg orbital. This also explains the observation in Fig. 2 that the electronic effect does not greatly depend on the geometrical structure of the molecule. Given that all of the measured structural evolution occurs on the Rydberg manifold[19], the electronic contribution to the signal can be treated as approximately constant throughout the dynamics. As a consequence, it is possible to separate the electronic and nuclear effects on the scattering patterns and to treat their contributions to the signal as approximately additive.

Structural determination analysis. To determine the transient molecular structures and construct the time-dependent video of the dynamical motions, the experimental signal at each time point was compared against a large set of scattering patterns computed from many hypothetical structures. This large pool of possible structures was created by extracting structures from a large and diverse set of surface-hopping trajectories propagated on the ground and excited Rydberg electronic states with the excess kinetic energy from the excitation taken into consideration. Approximately one million molecular geometries were extracted from the simulations. These sample a large conformational space that is confined to energetically allowed conformations that could potentially be accessed by the molecule during the dynamics. For each molecular structure, a scattering pattern was computed by approximating the geometrical structure using the Independent Atom Model[29] and adding the contribution of the electronic excitation of the planar structure in the 3*s* state (Fig. 2). By comparing the experimental signal with theoretical patterns, the least-squares fitting errors of all theoretical patterns from the pool were obtained at each time point. These errors were then plotted against each structural parameter; that is, the interatomic distances and the bond angles. In general, we found that the least-squares error varies as a function of any given structural parameter in a normal or skewed-normal distribution. The peak centres of these distributions are taken to represent the best-fitting structural parameters (see Supplementary Section 2 for details). This analysis gives the transient molecular structure at each time point independently, so that the measurement of many time points yields the time-dependent motions of the excited-state molecule. The analysis results in the probability of the laser exciting the molecules to the upper electronic state. This global, time-independent parameter was determined to be 5.7%, a value that gives confidence that multiphoton excitation processes do not interfere with our analysis.

After the damping of the observed oscillations is complete, the difference scattering signals settle to an essentially constant value. As the internal conversion from the $3p_z$ to the 3*s* state is complete after ~0.5 ps, the scattering signal at long delay times arises from the structure of NMM in the 3*s* Rydberg state. The excited-state structure of NMM—determined from experimental signals at long delay times (2.6–3.9 ps)—is given in Table 1. As the determination of the molecular structure is performed independently for each of the 25 time points, the structural parameters obtained from each of those time points are independent measurements that can be used to assess the precision of the structure determination. The errors reported in Table 1 are the standard deviations over measurements of independent time points. It is seen that the nearest-neighbour bond distances determined from this procedure have errors on the order of ~10 mÅ. To assess the accuracy of the result, Table 1 includes the optimized structure of NMM in its cation ground state. Although the ion structure is not necessarily identical to the structure in the 3*s* Rydberg state, it is probably quite similar, and Table 1 shows a reasonable agreement. The most notable difference between the ion minimum-energy structure and the vibrationally hot Rydberg excited-state structure seems to be in the low-frequency angular modes that are likely to be most affected by the high internal energy of the NMM molecule after internal conversion.

To ensure that the pool of possible molecular structures was sufficiently diverse, a second pool of structures was generated on the basis of a combination of comparatively low-level density functional theory and Hartree–Fock classical trajectories propagated on the ground state of the cation of NMM. As the topology of the cationic state of the molecule is expected to be similar to that of the Rydberg states of the neutral molecule, the conformational spaces constructed from the two are also expected to be similar. The results using this second pool (under the ion-surface dynamics pool column in Table 1) generally agree favourably with the high-level computation result (under the Rydberg-surface dynamics pool column in Table 1). The small discrepancy shown in torsional angles from

two different pools is mainly due to the substantially smaller number of geometries used in the ion-surface dynamics pool compared with the Rydberg-surface dynamics pool (further details in the Methods). This leads to a much lower local structure density around the true structure contained in the ion-surface pool compared to the Rydberg-surface pool. The consistency of the results obtained using the different pools demonstrates that the determination of molecular structures is robust with respect to the method used to generate the pool of structures. It should be noted, however, that because the calculated percent difference scattering pattern requires a simulated ground state scattering pattern as a reference, our method does depend on an accurate ground-state input structure. Given that the excited-state structure we determine is in good agreement with the calculated structure of the ground-state ion (Table 1), the ground-state input structure is inferred to be quite accurate.

Analysis of the structural dynamics. Given the ability to determine precise excited state molecular structures for each time point, we are now in a position to assemble a graphical representation of the time-dependent molecular structures in the form of a molecular movie. For this illustration, the geometry that gives the smallest-fit errors across all 21 non-hydrogenic interatomic distances is chosen as the representative geometry. By stitching together the images at each time point, the dynamical motions of the vibrating molecule are obtained (an animation is shown in Supplementary Video 2). An examination of the time dependence of some select structural parameters (Fig. 3) reveals the source of the dynamics observed in the experimental difference scattering pattern. Analysis of individual structural parameters indicates that the transient signal is dominated by signals arising from interatomic distances that involve the heavier atoms (rather than hydrogen atoms), which change following excitation (these include all of the distances between C5 and the other heavy atoms, as well as the O–N distance). Selected representative time-dependent structural parameters are fitted to a dynamical model that includes the contributions described above. The O–N–C5 angle (refer to Fig. 1 for atom labels) has an oscillatory period of 619 ± 22 fs, whereas the C5–N–C4–C3 torsional angle oscillates with a 613 ± 14 fs period. Both of these values are in good agreement with the fits to the overall scattering signal oscillation period of 623 ± 19 fs, and the previous photoelectron spectroscopic measurement at 208 nm (630 ± 13 fs)[19]. This indicates that the primary driver of the observed oscillation is the planarization motion of the amine group. For comparison, Fig. 3 includes the time dependence of the C2–C1–C4–C3 torsional angle, which does not participate in this motion. This torsional angle remains essentially unchanged during vibrational motion.

The time-dependent molecular structures also reveal that the oscillation in O–N–C5 angle dephases with an exponential time constant of 1,490 ± 785 fs, whereas the C5–N–C4–C3 torsional angle dephases in 1,900 ± 876 fs. Both of these time constants are larger than the damping in the overall signal intensity (635 ± 116 fs), although we note the relatively large errors in these determined values (see Supplementary Section 1 for details). This suggests that the decomposition of the overall scattering signals into specific, time-dependent geometrical parameters allows a more comprehensive understanding of the oscillatory umbrella motion than direct dynamic analysis of the overall scattering signal. Although the umbrella motion drives the relaxation of energy into the bath of vibrational states, its coherence may persist for longer than previously thought, and longer than analysis of the overall signal intensity would suggest.

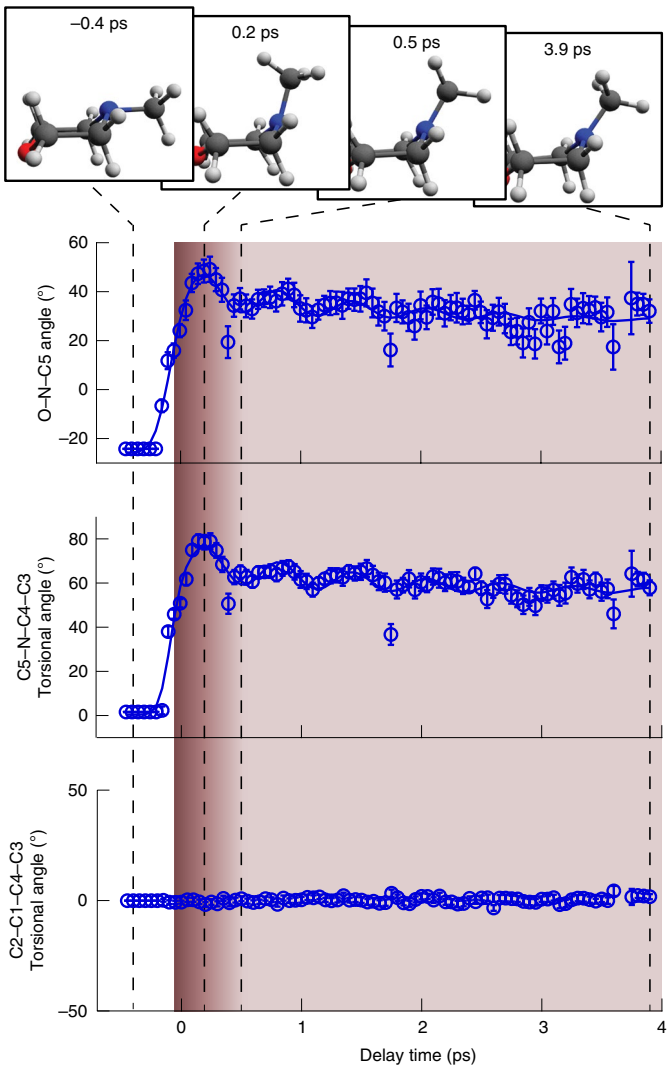

Fig. 3 | Time-dependent plots of selected structural parameters of NMM following Rydberg excitation. The O-N-C5 angle (top), the C5-N-C4-C3 torsional angle (middle) and the C2-C1-C4-C3 torsional angle (bottom), extracted from the structural determination as described in the text, are shown along with their respective 1σ error bars. The dynamic fits to the respective vibrational motions of the O-N-C5 angle and C5-N-C4-C3 torsional angle are also shown as solid lines. The approximate lifetime of the initially excited 3p_z Rydberg state (determined from photoelectron measurements in ref. [19]) is shown as a dark red shaded region, which corresponds to the 3s state when the colour is lighter. Example molecular structures for selected time points are also shown. A full animation is given in Supplementary Video 2.

Conclusions

In summary, we have captured transient molecular scattering signals that reveal the time-dependent excited-state molecular structure of NMM following Rydberg excitation. Precise molecular structures are obtained by reference to a large pool of potential structures generated computationally, with the resulting structures shown to be robust with respect to the choice of computational method. The resulting time-dependent molecular structure uncovers the vibrational motions in an excited polyatomic organic molecule. We observe large amplitude vibrations of the amine planarization mode and its dephasing on a picosecond timescale. It seems that the coherence of the vibrational motion survives the electronic relaxation[19] and persists for multiple vibrational periods. Although the overall signal intensity reflects the motions in many vibrational modes, and therefore has a faster apparent dephasing, the time dependence of specific structural parameters suggests that the intrinsic dephasing of the motions may be much slower than previously recorded.

The optical excitation in this instance is primarily a one-electron effect, and occurs on a background of the 56 electrons in the molecule. Because the scattering signals arise from the interference of scattering from different parts of the molecule, the excitation of a single electron leads to an effect on the scattering signal of about ~0.2% with the excitation fraction in the present experiment (Fig. 2), which is well within the experimental detection limit of ~0.05%. On the basis of our study, it is now conceivable that both vibrational structural motions and electron density changes can be observed during chemical reactions, which opens the door to observe (in real time) the formation and destruction of chemical bonds. Application to a variety of chemical reactions (including electrocyclic and charge transfer reactions) could provide previously unattainable experimental insights into chemical bonding and charge migration during reactions.

Methods

Experimental methods. The X-ray scattering measurements were performed in the coherent X-ray imaging instrument[30] at the LCLS[31] at the SLAC National Accelerator Laboratory. The 200 nm pump laser was the fourth harmonic of a 120 Hz Ti:sapphire laser with an ~80 fs pulse duration with ~1 μJ per pulse on target and a ~1.5 nm spectral bandwidth. The X-ray probe pulse was generated from LCLS, which operated at 120 Hz with ~10^{12} photons per pulse at 9.5 keV photon energy with a 20 eV full-width at half-maximum bandwidth and a ~30 fs pulse duration. The cross-correlation time of the pump and probe pulses was determined to be 89 ± 7 fs from the onset of the observed time-dependent scattering signals. The gaseous NMM sample pressure was controlled by a piezoelectric needle valve to ~7 torr of pressure at the interaction region. The gas cell and the CSPAD detector are in vacuum, with an average background pressure outside of the scattering cell of 2.6×10^{-4} torr, which is mostly comprised of the NMM that flows out of the windowless scattering cell. The pulse energy and gas pressure were optimized for a reduced background signal and a <10% excitation probability. The interaction length was kept small at 2.4 mm, which prevented excessive Beer–Lambert attenuation of the UV beam at the downstream end of the interaction region.

To collect time-resolved scattering patterns, the pump–probe delay time was controlled by a motorized delay stage, and the shot-to-shot timing jitter of the X-ray beam was monitored with a specialized timing tool[32]. The actual time delay of each shot was then determined to be the sum of the laser stage position and the edge position of the time tool. Furthermore, the shot-to-shot X-ray intensity was monitored by a photodiode downstream of the scattering cell. To achieve the necessary noise level (<0.1%), it was necessary to calibrate the intensity after the diffractometer set-up, because the X-ray also has spatial jitter that affects the transmission of the X-ray through the Pt pinholes (see Fig. 1).

The scattered X-rays were detected via a 2.3-megapixel CSPAD[24]. Details of the detector calibration, as well as the analysis of the measured scattering signals, are presented in Supplementary Section 1, as well as in the Supplementary Information of ref. [33].

Computational methods. To calculate the percent difference scattering signal caused by electronic excitation and by nuclear vibrational motions (see Fig. 2), the equatorial and axial geometries were optimized using the B3LYP/6-311++G(*d*,*p*) method for the neutral ground state, and the planar geometry was optimized using B3LYP/6-311++G(*d*,*p*) for the ionic ground state. The selected structural parameters of the optimized ionic ground state are shown in Table 1 in the ion structure column. The structure of the neutral ground-state equatorial geometry was further optimized at the CASSCF(2,5)/6-311+G(*d*) level and was used to simulate the ground-state scattering pattern as a reference. The selected structural parameters of the optimized neutral ground state are also presented in Table 1 in the ground-state structure column. The ab initio wavefunctions used to simulate the scattering patterns in the 3*s* and 3*p* states were calculated using the SA5-CAS(2,5)/6-311++G(*d*,*p*) method for the equatorial and planar NMM structures. All ab initio calculations were performed using the MOLPRO electronic structure software package[34,35], and scattering patterns were calculated using our own computer codes documented in refs. [27,28,36].

Using a total of 107 trajectories, we obtained approximately one million molecular geometries. We simulated the Rydberg-surface dynamics of photoexcited NMM using the SHARC[37–39] code interfaced with MOLPRO. SHARC treats nuclear motions classically, but non-adiabatic effects were included using the fewest-switches surface-hopping approach. The dynamics was propagated on the four lowest singlet electronic excitation states. The structures sampled from a Wigner distribution were initially populated to the 3*s* and three 3*p* states on the basis of their oscillator strengths, with 107 trajectories run for 1,000 fs. The electronic structure calculations during the dynamics were run at the SA5-CAS(2,5)/6-311+G(*d*) level of theory. A pool of 1,070,107 (greater than 10^6) geometries was extracted from the simulations. To test the dependence of the structure determination on the level of theory used, an ion-surface dynamics simulation was also performed. In this simulation, the nuclei are still treated classically, whereas electrons are treated quantum mechanically and calculated on the ion ground-state surface instead of the neutral Rydberg surfaces. We deliberately chose the ion surface rather than the Rydberg surface for this simulation to further test the independence of the resulting structure determination on the method used to create the pool of structures. In half of the trajectories, the UHF/6-311+G(*d*) method was used to calculate the ion state NMM at each time step, whereas in the other half, density functional theory (using the Perdew–Burke–Ernzerhof functional) was used instead. Combined, 173,997 geometries were obtained by the ion-surface dynamics simulations. Further details of the structural determination are included in Supplementary Section 2.

Data availability

The raw experimental data are archived on SLAC's internal file system. The raw pools of computed structures are stored locally at Brown University. All raw data are available from the corresponding author on reasonable request.

Code availability

The calculation of elastic scattering patterns from ab initio wavefunctions has been discussed in earlier publications[27,28,36]. The codes used to calculate scattering patterns, process the experimental data and perform the structural determination analysis are available from the corresponding author on reasonable request.

Received: 20 December 2018; Accepted: 10 June 2019;
Published online: 08 July 2019

References

1. Heller, E. J. Bound-state eigenfunctions of classically chaotic Hamiltonian systems: scars of periodic orbits. *Phys. Rev. Lett.* **53**, 1515–1518 (1984).
2. Tannor, D. J. *Introduction to Quantum Mechanics: A Time-dependent Perspective* (University Science Books, Sausalito, 2007).
3. Marcus, R. A. Electron transfer reactions in chemistry: theory and experiment. *Angew. Chem. Int. Ed.* **32**, 1111–1121 (1993).
4. Peirce, P., Dahleh, M. A. & Rabitz, H. Optimal control of quantum-mechanical systems: existence, numerical approximation, and applications. *Phys. Rev. A* **37**, 4950 (1988).
5. Zewail, A. H. Femtochemistry: atomic-scale dynamics of the chemical bond using ultrafast lasers (Nobel lecture). *Angew. Chem. Int. Ed.* **39**, 2586–2631 (2000).
6. Lambert, W. R., Felker, P. M. & Zewail, A. H. Quantum beats and dephasing in isolated large molecules cooled by supersonic jet expansion and excited by picosecond pulses: anthracene. *J. Chem. Phys.* **75**, 5958–5960 (1981).
7. Minitti, M. P. et al. Imaging molecular motion: femtosecond X-ray scattering of an electrocyclic chemical reaction. *Phys. Rev. Lett.* **114**, 255501 (2015).
8. Glownia, J. M. et al. Self-referenced coherent diffraction X-ray movie of ångstrom- and femtosecond-scale atomic motion. *Phys. Rev. Lett.* **117**, 153003 (2016).
9. Küpper, J. et al. X-ray diffraction from isolated and strongly aligned gas-phase molecules with a free-electron laser. *Phys. Rev. Lett.* **112**, 083002 (2014).
10. Barty, A., Küpper, J. & Chapman, H. N. Molecular imaging using X-ray free-electron lasers. *Annu. Rev. Phys. Chem.* **64**, 415–435 (2013).
11. Harb, M. et al. Electronically driven structure changes of Si captured by femtosecond electron diffraction. *Phys. Rev. Lett.* **100**, 155504 (2008).
12. Ischenko, A. A., Weber, P. M. & Dwayne Miller, R. J. Capturing chemistry in action with electrons: realization of atomically resolved reaction dynamics. *Chem. Rev.* **117**, 11066–11124 (2017).
13. Yang, J. et al. Diffractive Imaging of coherent nuclear motion in isolated molecules. *Phys. Rev. Lett.* **117**, 153002 (2016).
14. Yang, J. et al. Imaging CF_3I conical intersection and photodissociation dynamics with ultrafast electron diffraction. *Science* **361**, 64–67 (2018).
15. Zewail, A. H. 4D ultrafast electron diffraction, crystallography, and microscopy. *Annu. Rev. Phys. Chem.* **57**, 65–103 (2006).
16. Budarz, J. M. et al. Observation of femtosecond molecular dynamics via pump–probe gas phase x-ray scattering. *J. Phys. B* **49**, 34001 (2016).
17. Minitti, M. P. et al. Toward structural femtosecond chemical dynamics: imaging chemistry in space and time. *Faraday Discuss.* **171**, 81–91 (2014).
18. Williamson, J. C., Cao, J., Ihee, H., Frey, H. & Zewail, A. H. Clocking transient chemical changes by ultrafast electron diffraction. *Nature* **386**, 159–162 (1997).
19. Zhang, Y., Jónsson, H. & Weber, P. M. Coherence in nonradiative transitions: internal conversion in Rydberg-excited *N*-methyl and *N*-ethyl morpholine. *Phys. Chem. Chem. Phys.* **19**, 26403–26411 (2017).
20. Waters, M. D. J. et al. Symmetry controlled excited state dynamics. *Phys. Chem. Chem. Phys.* **21**, 2283–2294 (2019).
21. Yong, H. et al. Determining orientations of optical transition dipole moments using ultrafast X-ray scattering. *J. Phys. Chem. Lett.* **9**, 6556–6562 (2018).

22. Zhang, Y., Deb, S., Jónsson, H. & Weber, P. M. Observation of structural wavepacket motion: the umbrella mode in Rydberg-excited N-methyl morpholine. *J. Phys. Chem. Lett.* **8**, 3740–3744 (2017).
23. Dsouza, R., Cheng, X., Li, Z., Miller, R. J. D. & Kochman, A. Oscillatory photoelectron signal of *N*-methylmorpholine as a test case for the algebraic-diagrammatic construction method of second order. *J. Phys. Chem. A* **122**, 9688–9700 (2018).
24. Philipp, H. T., Hromalik, M., Tate, M., Koerner, L. & Gruner, S. M. Pixel array detector for X-ray free electron laser experiments. *Nucl. Instrum. Methods Phys. Res. A* **649**, 67–69 (2011).
25. Baskin, J. S. & Zewail, A. H. Ultrafast electron diffraction: oriented molecular structures in space and time. *ChemPhysChem* **6**, 2261–2276 (2005).
26. Lorenz, U., Møller, K. B. & Henriksen, N. E. On the interpretation of time-resolved anisotropic diffraction patterns. *New J. Phys.* **12**, 113022 (2010).
27. Northey, T., Zotev, N. & Kirrander, A. Ab initio calculation of molecular diffraction. *J. Chem. Theory Comput.* **10**, 4911–4920 (2014).
28. Northey, T., Moreno Carrascosa, A., Schäfer, S. & Kirrander, A. Elastic X-ray scattering from state-selected molecules. *J. Chem. Phys.* **145**, 154304 (2016).
29. Warren, B. E. *X-ray Diffraction* (Courier Corporation, 1969).
30. Liang, M. et al. The coherent X-ray imaging instrument at the Linac coherent light source. *J. Synchrotron Radiat.* **22**, 514–519 (2015).
31. Emma, P. et al. First lasing and operation of an ångstrom-wavelength free-electron laser. *Nat. Photon.* **4**, 641–647 (2010).
32. Bionta, M. R. et al. Spectral encoding method for measuring the relative arrival time between X-ray/optical pulses. *Rev. Sci. Instrum.* **85**, 083116 (2014).
33. Ruddock, J. M. et al. Simplicity beneath complexity: counting molecular electrons reveals transients and kinetics of photodissociation reactions. *Angew. Chem. Int. Ed.* **58**, 6371–6375 (2019).
34. Werner, H. J. et al. MOLPRO v.2012.1 (Molpro, 2012); https://www.molpro.net
35. Werner, H. J., Knowles, P. J., Knizia, G., Manby, F. R. & Schütz, M. Molpro: a general-purpose quantum chemistry program package. *WIREs Comput. Mol. Sci.* **2**, 242–253 (2012).
36. Moreno Carrascosa, A., Northey, T. & Kirrander, A. Imaging rotations and vibrations in polyatomic molecules with X-ray scattering. *Phys. Chem. Chem. Phys.* **19**, 7853–7863 (2017).
37. Mai, S. et al. SHARC v.2.0 (SHARC, 2018); https://sharc-md.org
38. Mai, S., Marquetand, P. & González, L. Nonadiabatic dynamics: the SHARC approach. *WIREs Comput. Mol. Sci.* **8**, 1370 (2018).
39. Richter, M., Marquetand, P., González-Vázquez, J., Sola, I. & González, L. SHARC: ab initio molecular dynamics with surface hopping in the adiabatic representation including arbitrary couplings. *J. Chem. Theory Comput.* **7**, 1253–1258 (2011).

Acknowledgements

The authors thank G. Stewart (SLAC National Accelerator Laboratory) for his generous assistance with preparing the figures. This work was supported by the US Department of Energy, Office of Science, Basic Energy Sciences, under award no. DESC0017995, and by the Army Research Office (grant no. W911NF-17-1-0256). Use of the LCLS, SLAC National Accelerator Laboratory, is supported by the US Department of Energy, Office of Science, Office of Basic Energy Sciences under contract no. DE-AC02-76SF00515.

Author contributions

P.M.W., A.K. and M.P.M. directed the project. M.L. and S.B. performed X-ray alignment and data collection. S.C., J.S.R. and M.P.M. performed laser alignment. T.J.L. and J.E.K. provided software support during the experiment. W.D. and Y.C. performed record keeping during the experiment. B.S., H.Y., N.Z., J.R., N.G., Y.C. and W.D. performed analyses on the experimental data. H.Y., N.Z. and D.B. performed theoretical computations and structural-determination analysis. B.S. planned the detailed experiments and implemented the data analysis. B.S. and H.Y. wrote the manuscript in consultation with the other authors.

Competing interests

The authors declare no competing interests.

Additional information

Supplementary information is available for this paper at https://doi.org/10.1038/s41557-019-0291-0.

Reprints and permissions information is available at www.nature.com/reprints.

Correspondence and requests for materials should be addressed to P.M.W.

Publisher's note: Springer Nature remains neutral with regard to jurisdictional claims in published maps and institutional affiliations.